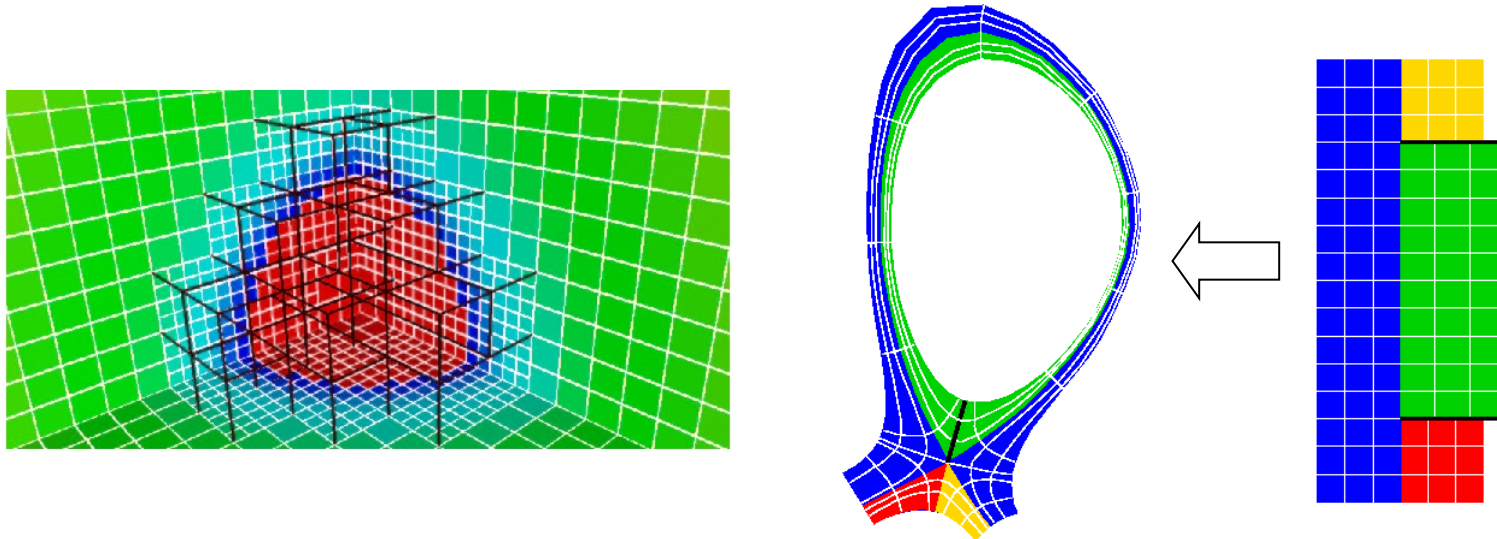# High-Order Finite-Volume Methods

Phillip Colella

Computational Research Division
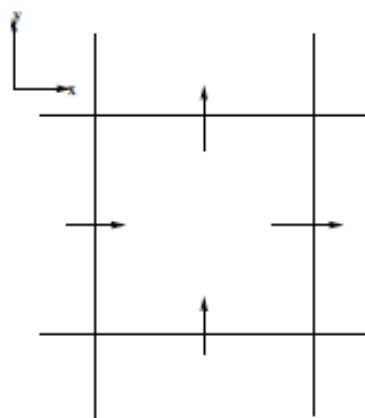
Lawrence Berkeley National Laboratory

Why Higher Order ?

- Locally-refined grids, mapped-multiblock grids – smooth except at boundaries between different refinement levels / blocks. Leads to loss of one order of accuracy at boundaries: $2^{nd} \rightarrow 1^{st}$, $4^{th} \rightarrow 3^{rd}$.

- Over the next decade, bytes / flop expected to go down by 10x. Similar relative increases in imbalance between communication and computation (higher latencies, lower bandwidth). Want to do more computation per unit of data access, use less data overall.

BERKELEY LAB
LAWRENCE BERKELEY NATIONAL LABORATORY

U.S. DEPARTMENT OF ENERGY | Office of Science

Finite-Volume Methods on Structured Grids

We use the divergence theorem for computing the average of div(F) over a control volume.

$$-\frac{1}{h^D}\int_{V_i}\nabla\cdot\vec{F}d\boldsymbol{x}=-\frac{1}{h}\sum_d\langle F^d\rangle_{\boldsymbol{i}+\frac{1}{2}\boldsymbol{e}^d}-\langle F^d\rangle_{\boldsymbol{i}-\frac{1}{2}\boldsymbol{e}^d}$$

$$\langle F^d\rangle_{\boldsymbol{i}+\frac{1}{2}\boldsymbol{e}^d}\equiv\frac{1}{h^{D-1}}\int_{A_d^{\pm}}F^d(\boldsymbol{x},t)dA$$

• This is an exact relationship – the approximations are introduced by the choice of quadrature for the face integrals.
• For smooth grids, the truncation error of the approximation to the average of div(F) is the same as the truncation the error in the flux (standard centered-difference error cancellation applies here as well).

Design Issues for High-Order Finite-Volume Methods

- High-order quadratures for fluxes.

- Time-dependent problems: time discretizations, limiters for hyperbolic problems, semi-implicit methods.

- Adaptive mesh refinement.

- Extension to mapped grids, multiblock grids.

High-Order Quadratures for Fluxes

At second-order accuracy, can approximate averages by the midpoint rule. For higher-order accuracy, must distinguish between cell averages, face averages, and point values.

$$\langle F^d \rangle_{i \pm \frac{1}{2} e^d} = \frac{1}{h^{D-1}} \int_{A_d^{\pm}} F^d \, dA,$$

$$\langle F^d \rangle = F^d(x_0) + \frac{h^2}{24} \sum_{d' \neq d} \frac{\partial^2 F_d}{\partial x_{d'}^2} + O(h^4)$$

$$\langle fg \rangle_i = \langle f \rangle_i \langle g \rangle_i + \frac{h^2}{12} \nabla f \cdot \nabla g + O(h^4)$$

$$\langle fg \rangle_{i + \frac{1}{2} e^d} = \langle f \rangle_{i + \frac{1}{2} e^d} \langle g \rangle_{i + \frac{1}{2} e^d} + \frac{h^2}{12} \sum_{d' \neq d} \frac{\partial f}{\partial x_{d'}} \frac{\partial g}{\partial x_{d'}} + O(h^4)$$

These can be used to compute more general nonlinear functions:

$$\langle W(U) \rangle = W(\langle U \rangle) + O(h^2)$$

$$U_i = \langle U \rangle_i - \frac{h^2}{24} \Delta^{(2)} \langle U \rangle_i \qquad W_i = W(U_i) \qquad \langle W \rangle_i = W_i + \frac{h^2}{24} \Delta^{(2)} \overline{W}_i. \qquad \overline{W}_i = W(\langle U \rangle_i)$$

"Convolution / deconvolution" Ref: Barad and Colella, 2005

BERKELEY LAB
LAWRENCE BERKELEY NATIONAL LABORATORY

U.S. DEPARTMENT OF ENERGY | Office of Science

Semi-Discrete Formulation of Finite-Volume Methods for Time-Dependent Problems

We can integrate conservation laws

$$\frac{\partial U}{\partial t} + \nabla \cdot \vec{F} = 0$$

over rectangular control volumes

$$V_{\boldsymbol{i}} = [\boldsymbol{i}h, (\boldsymbol{i} + \boldsymbol{u})h] \ , \ \boldsymbol{i} \in \mathbb{Z}^D \ , \ \boldsymbol{u} = (1, 1, \dots, 1)$$

to obtain a system of ordinary differential equations

$$\frac{d\langle U \rangle_{\boldsymbol{i}}}{dt} = -\frac{1}{h^D} \int_{V_{\boldsymbol{i}}} \nabla \cdot \vec{F} d\boldsymbol{x} = -\frac{1}{h} \sum_d \langle F^d \rangle_{\boldsymbol{i}+\frac{1}{2}\boldsymbol{e}^d} - \langle F^d \rangle_{\boldsymbol{i}-\frac{1}{2}\boldsymbol{e}^d}$$

$$\langle U \rangle_{\boldsymbol{i}} \equiv -\frac{1}{h^D} \int_{V_{\boldsymbol{i}}} U(\boldsymbol{x}, t) d\boldsymbol{x} \quad \langle F^d \rangle_{\boldsymbol{i}+\frac{1}{2}\boldsymbol{e}^d} \equiv \frac{1}{h^{D-1}} \int_{A_d^\pm} F^d(\boldsymbol{x}, t) dA$$

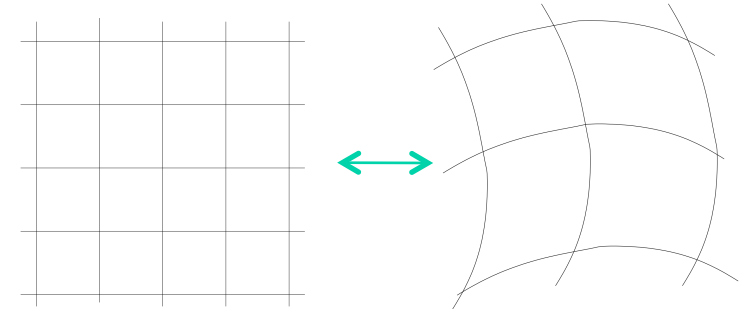We use a method of lines approach, separating spatial and temporal discretization.

High-Order Finite-Volume Methods on Mapped Grids

We assume that we have a smooth mapping from an abstract coordinate space to physical space:

$$\mathbf{x} = \mathbf{X}(\xi) \ , \ \mathbf{X} : [0,1]^D \to \mathbf{R}^D$$

$$\nabla_{\mathbf{x}} \cdot \vec{F} \equiv \frac{1}{J} \nabla_\xi \cdot (\mathbf{N}^T \vec{F})$$

$$J \equiv det(\nabla_\xi \mathbf{X}) \ , \ \mathbf{N}_{p,q} = det((\nabla_\xi \mathbf{X})(p|\mathbf{e}^q))$$

Finite-volume discretization: if V_i is a rectangular cell in the mapping space,

$$\frac{1}{h^D} \int_{V_i} \nabla \cdot (\boldsymbol{N}^T \vec{F}) d\boldsymbol{\xi} = -\frac{1}{h} \sum_{d=1}^{D} \langle (\boldsymbol{N}^T \vec{F})_d \rangle_{\boldsymbol{i}+\frac{1}{2}\boldsymbol{e}^d} - \langle (\boldsymbol{N}^T \vec{F})_d \rangle_{\boldsymbol{i}-\frac{1}{2}\boldsymbol{e}^d}$$

Fourth-order accurate approximation to face integrals:

$$\langle (\boldsymbol{N}^T \vec{F})_d \rangle_{\boldsymbol{i}+\frac{1}{2}\boldsymbol{e}^d} = \left(\langle \boldsymbol{N}^T \rangle_{\boldsymbol{i}+\frac{1}{2}\boldsymbol{e}^d} \langle \vec{F} \rangle_{\boldsymbol{i}+\frac{1}{2}\boldsymbol{e}^d} \right)_d + \frac{h^2}{12} \sum_{d' \neq d} \left(\frac{\partial}{\partial \xi_{d'}}(\boldsymbol{N}^T) \cdot \frac{\partial}{\partial \xi_{d'}}(\vec{F}) \right)_d + O(h^4)$$

Guarantee freestream preservation by using the Poincare lemma:

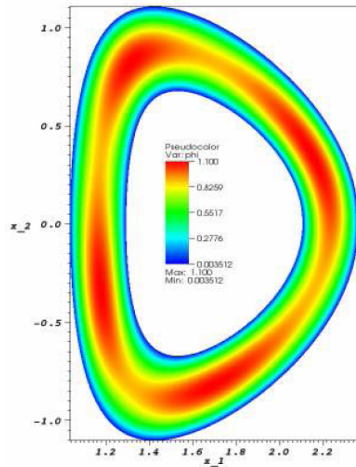$$\nabla_{\boldsymbol{\xi}} \cdot N^s = 0 \implies \int_{A_d} N_d^s dA_\xi = \sum_{\pm=+,-} \sum_{d' \neq d} \pm \int_{E_{d,d'}^\pm} \mathcal{N}_{d,d'}^s dE_\xi$$
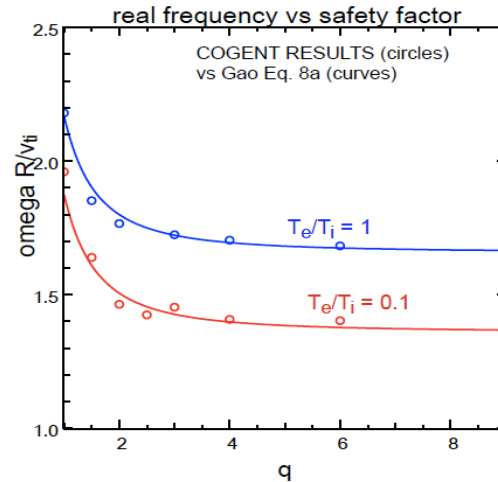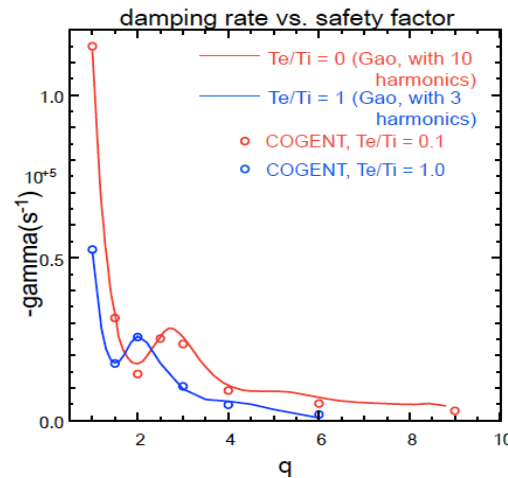
Can use any high-order quadrature to compute edge integrals

Ref: Colella, Dorr, Hittinger and Martin, 2010

BERKELEY LAB
LAWRENCE BERKELEY NATIONAL LABORATORY

U.S. DEPARTMENT OF ENERGY | Office of Science

Gyrokinetic Plasma Models in 4D

Advection in 4D phase space, coupled to the solution to an elliptic equation in physical space.

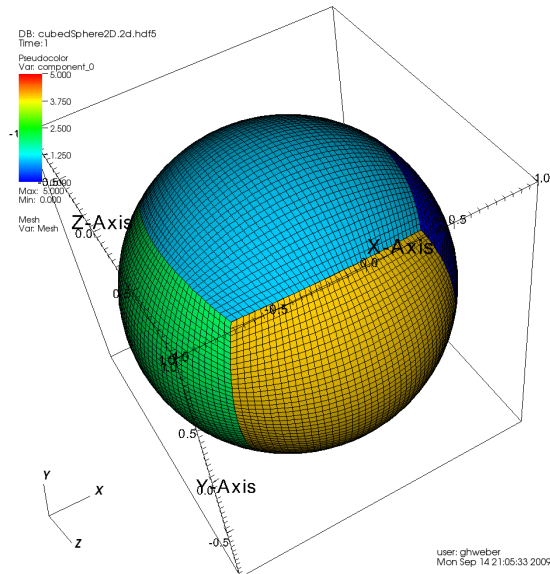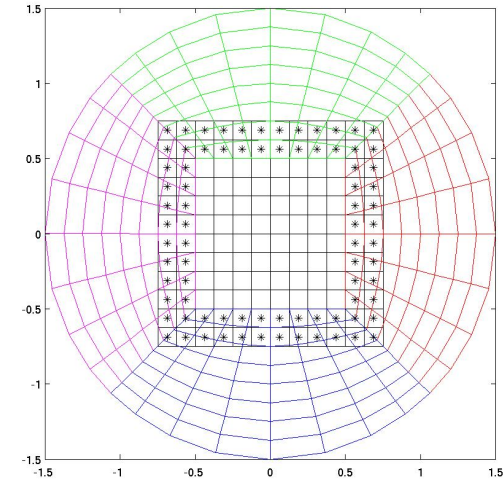| Grid refinement level N	Grid $(r \times \theta \times v_\parallel \times \mu)$	Estimated density error conv. rate ρ_N	Richardson extrapolated density error ϵ_N
1	$8 \times 32 \times 32 \times 8$		
2	$16 \times 64 \times 64 \times 16$		
3	$32 \times 128 \times 128 \times 32$	3.8 (L1)	3.37×10^{-7} (L1)
		3.8 (L2)	6.03×10^{-7} (L2)
		4.1 (Max)	1.95×10^{-4} (Max)
4	$64 \times 256 \times 256 \times 64$	4.2 (L1)	1.40×10^{-8} (L1)
		4.1 (L2)	2.95×10^{-7} (L2)
		3.6 (Max)	1.69×10^{-5} (Max)

Ref: Dorr, et al., 2010

Mapped Multiblock Grids

Use polynomial interpolation and least-squares to obtain ghost-cell values:

$$\varphi(\boldsymbol{x}) \approx \sum_{\boldsymbol{p}} a_{\boldsymbol{p}} \boldsymbol{x}^{\boldsymbol{p}} \ , \ \boldsymbol{x}^{\boldsymbol{p}} = \prod_{d=1}^{D} x_d^{p_d}$$

$$\int_{V_{\boldsymbol{v}}} \varphi(\boldsymbol{x}) d\boldsymbol{x} = \sum_{\boldsymbol{p}} a_{\boldsymbol{p}} \int_{V_{\boldsymbol{v}}} \boldsymbol{x}^{\boldsymbol{p}} d\boldsymbol{x} \ , \ \boldsymbol{v} \in \mathcal{V}$$
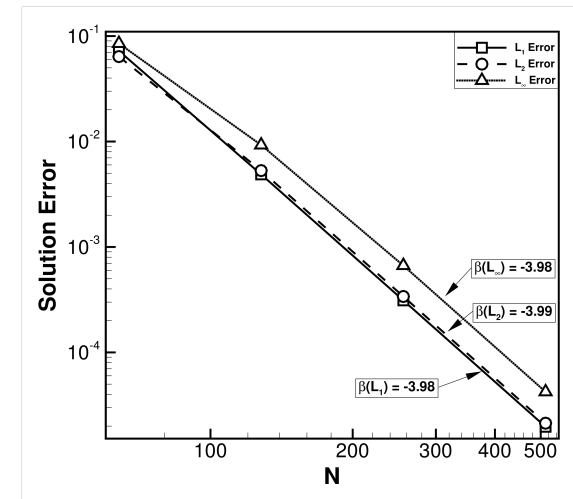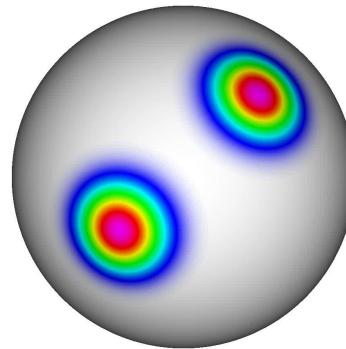
Ref: Johansen, McCorquodale, Ullrich, and Colella, in preparation

Adaptive Mesh Refinement for Hyperbolic Problems

A straightforward generalization of the second-order accurate finite-volume AMR methods. Most of the changes are for interpolation at refinement boundaries.

• Derive fourth-order accurate time interpolation from dense output of Runge-Kutta method on next coarser level. In the presence of limiters, it is essential that the time interpolation include a representation of the truncation error for the substages of Runge-Kutta.

• Fourth-order spatial interpolation coefficients derived from least-squares method similar to that for multiblock.

• For mapped grids we use a generalization to higher order of the methods developed for the second-order case to maintain conservation and freestream preservation across levels.
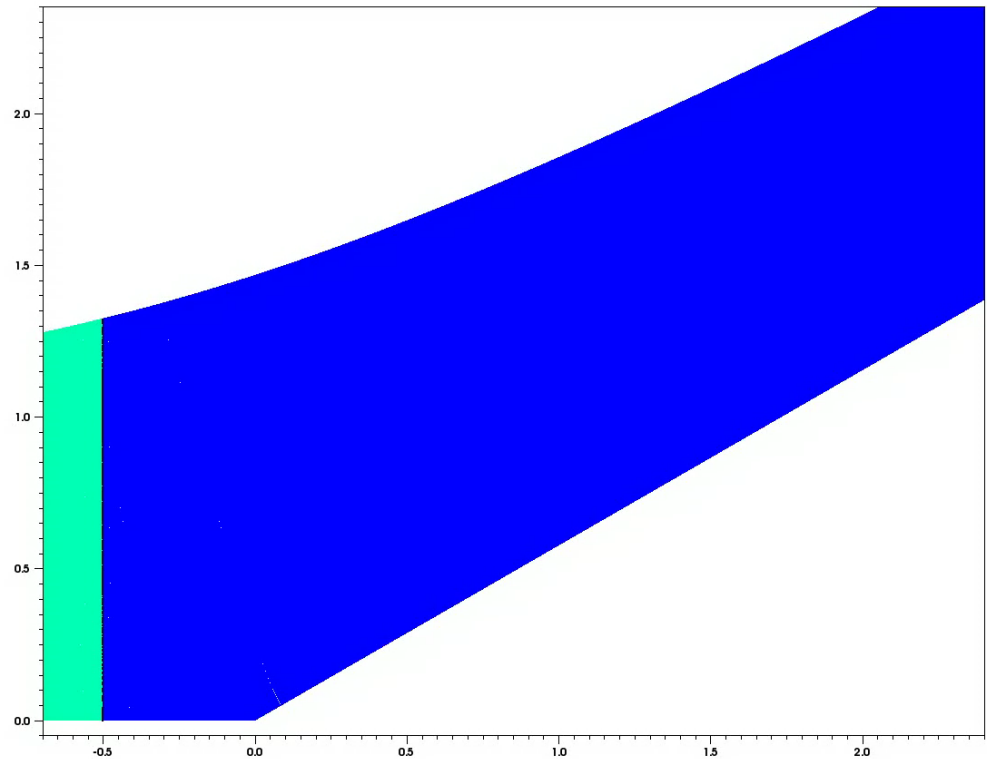
Ref: McCorquodale and Colella, 2011; Guzik, McCorquodale, and Colella, 2012.

limiter	1/64: 1/128	rate	1/128: 1/256	rate	1/256: 1/512	rate	1/512: 1/1024
on	7.29e-06	3.97	4.66e-07	3.95	3.01e-08	3.99	1.90e-09
off	7.29e-06	3.97	4.66e-07	3.95	3.01e-08	3.99	1.90e-09

BERKELEY LAB
LAWRENCE BERKELEY NATIONAL LABORATORY

U.S. DEPARTMENT OF ENERGY | Office of Science

Extremum-Preserving Limiters

Approach used above: centered differences, geometric limiting applied at each stage of RK. At extrema, compare different estimates of second derivatives to determine degree of limiting.

Issues:

• Geometric limiting at each stage -> time step limited by donor cell, scales like 1/(Dimension).

• Centered differencing is dissipation-free, interaction with RK + stage-wise limiters is brittle.

• Alternative approach:

  – Use upstream-centered differencing for high-order method.

  – Apply 1979 Zalesak extremum-preserving FCT to the sum of the fluxes at the end of the time step; leaves us free to choose low-order method (e.g. corner-coupled upwind methods).

  – Compute bounds on extrema using local quadratic interpolation.

Upstream-Centered Differencing

$$\frac{\partial \rho}{\partial t} + \frac{\partial \rho}{\partial x} = 0$$

$$\rho_{j+\frac{1}{2}} = \frac{1}{60}(\rho_{j-2} - 8\rho_{j-1} + 37\rho_j + 37\rho_{j+1} - 8\rho_{j+2} + \rho_{j+3}) \; \text{(Centered)}$$

$$= \frac{1}{60}(-\rho_{j-3} + 7\rho_{j-2} - 23\rho_{j-1} + 57\rho_j + 22\rho_{j+1} - 2\rho_{j+2}) \qquad \text{(Upstream-Centered)}$$

Both are sixth-order accurate approximations to $\quad \left. \frac{\partial}{\partial x} \int^{x} \rho(x',t)dx' \right|_{(j+\frac{1}{2})\Delta x}$
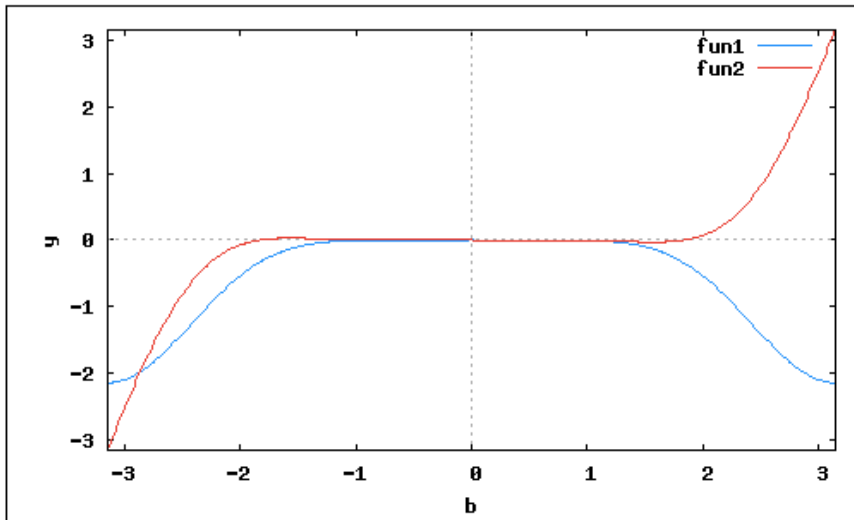
Von Neumann analysis of upstream-centered operator.
Red - imaginary part of the error.
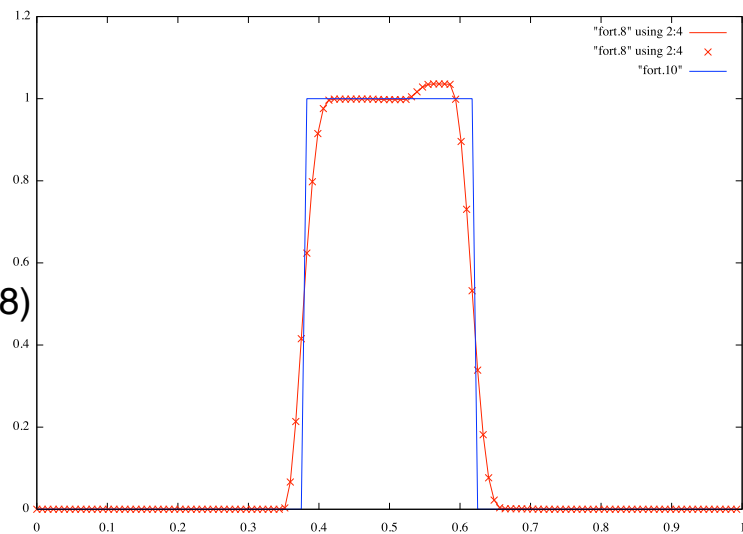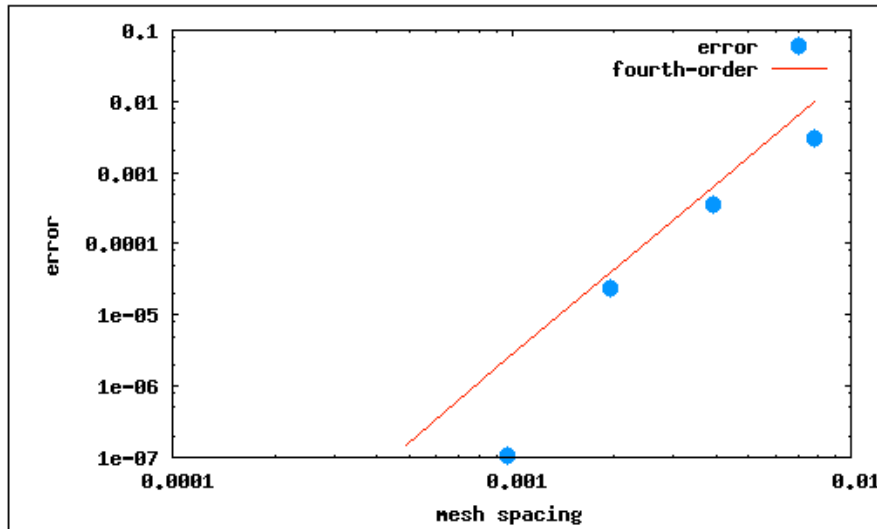Blue - real part of the error.

Example: Square Wave, CFL=.1

Centered
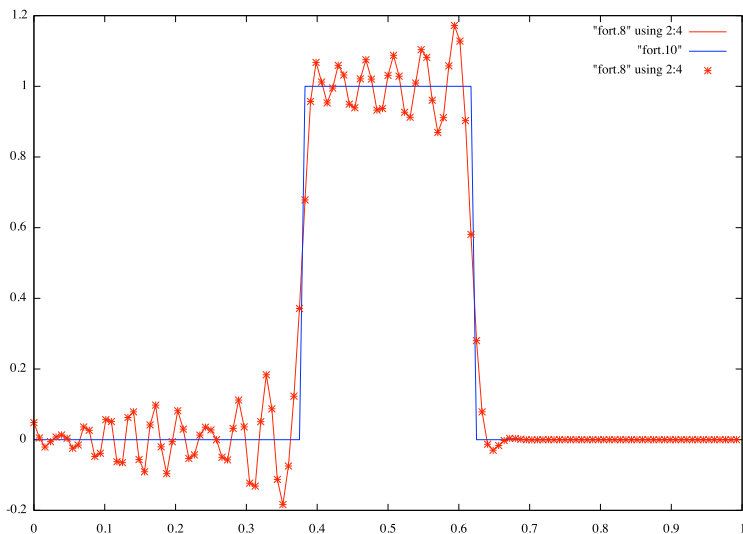
Upstream-centered
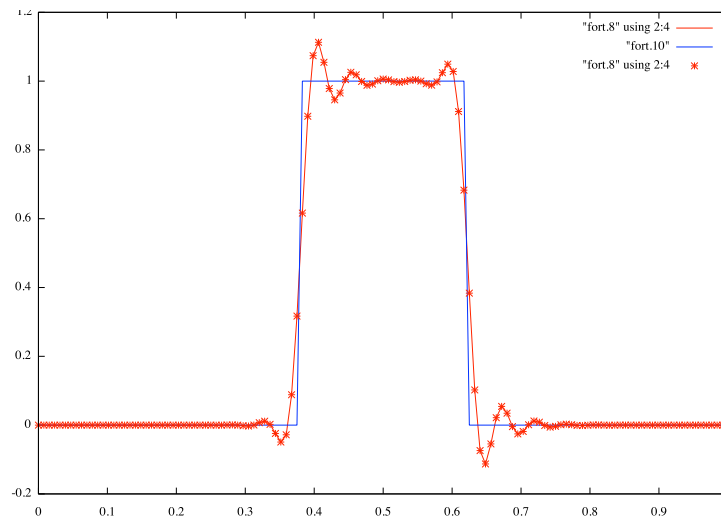
No limiter
(T = 1,N=256)
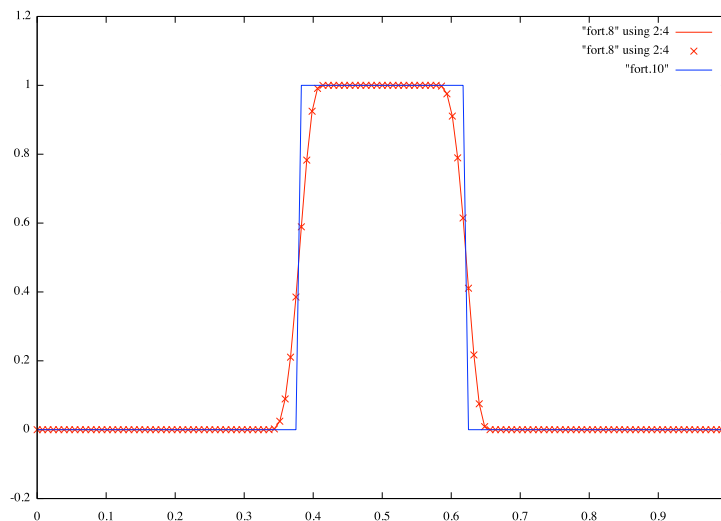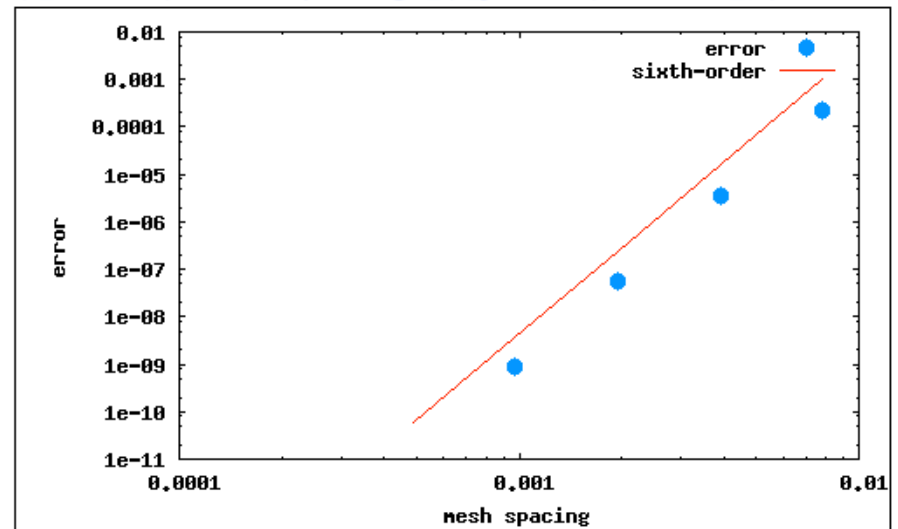
Limiter
(T = 10, N=128)

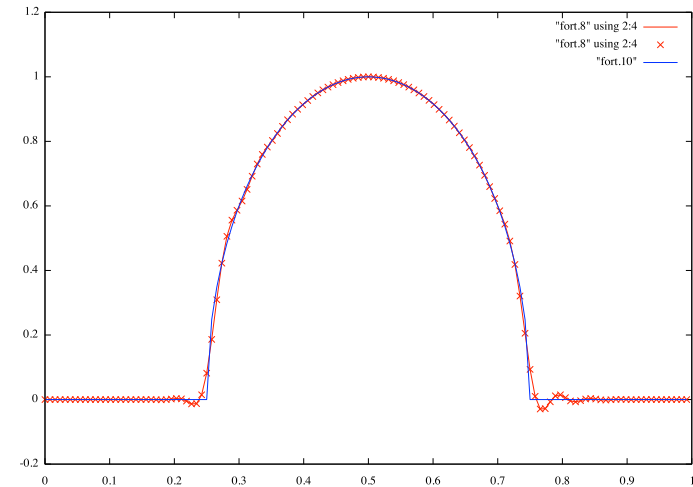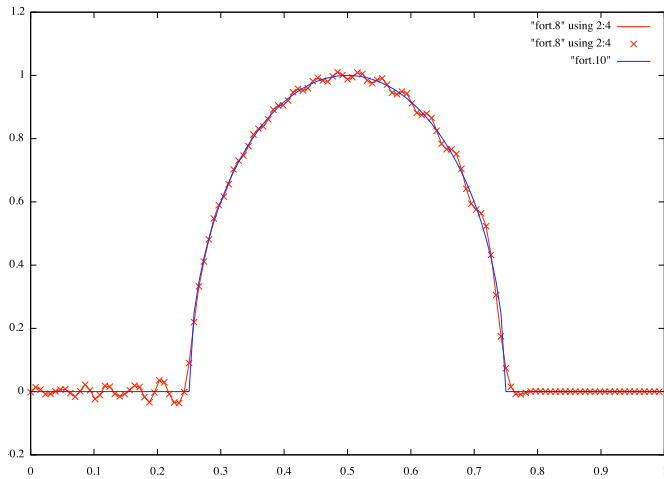# Convergence for Gaussian initial Data (Upstream-Centered, with Limiter)

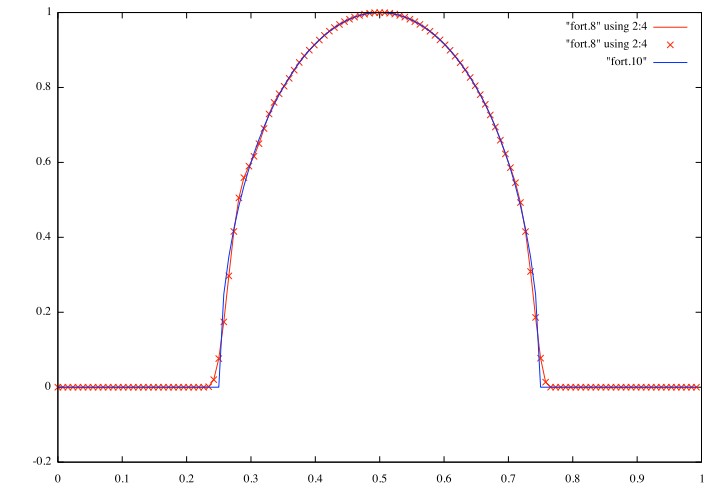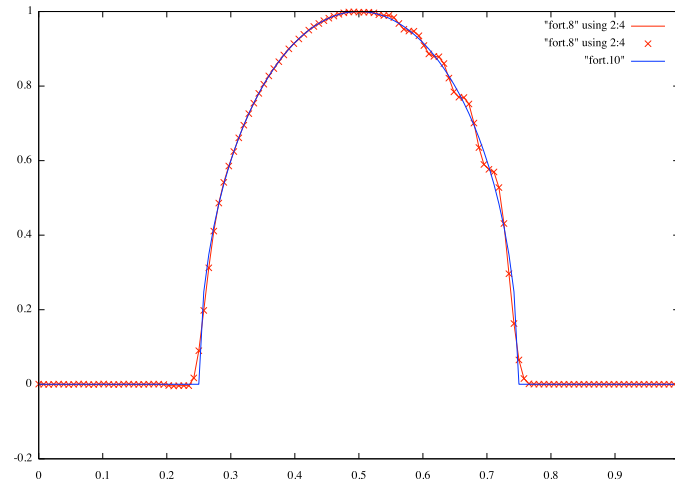T=1, CFL = .8

T=1, CFL = .1

Example: Semicircle, CFL=.1

Centered

Upstream-centered

No limiter

limiter

BERKELEY LAB
LAWRENCE BERKELEY NATIONAL LABORATORY

U.S. DEPARTMENT OF ENERGY | Office of Science

Conclusions and Future Work

Ongoing work:

• Extend upstream-centered method to multiple dimensions.

• Positivity preservation using redistribution.

• Ongoing applications development: incompressible Navier-Stokes, kinetic problems in plasmas, atmospheric modeling for climate, Maxwell's equations.

• Use of ARK methods for semi-implicit treatment of stiff terms.

• Extension of cut-cell methods to higher order.

Final comments:

• Classical methods (von Neumann analysis) still provide insight (e.g. Paul Ullrich's paper on comparison of methods for the wave equation).

• Basic framework for designing methods for discontinuous solutions to hyperbolic conservation laws developed in the late 1970's - early 1980's remains applicable to new settings, new requirements.

BERKELEY LAB
LAWRENCE BERKELEY NATIONAL LABORATORY

U.S. DEPARTMENT OF ENERGY | Office of Science